

# Preparation and investigation of binder-free TiO<sub>2</sub> paste for low temperature flexible DSSC applications

H. KANBUR CAVUS\*, R. SAHINGOZ

*Department of Physics, Yozgat Bozok University, Yozgat, 66900, Turkey*

In this study, for the production of flexible photoanodes, a binder-free TiO<sub>2</sub> paste has been prepared. The photoelectrodes fabricated with this paste at low temperature have been achieved a very good contact compared to the results prepared by conventional high temperature procedures. These flexible photoanodes have been sensitized with Ruthenizer N719 dye at 24 hours and this flexible photoanode and Pt counter electrode have been combined. The characteristic values of J<sub>sc</sub>, V<sub>oc</sub>, FF and conversion efficiency (η) have been obtained 20.9 mA/cm<sup>2</sup>, 671 mV, 0.57, and 7.95 % respectively for the flexible dye sensitized solar cell (DSSC).

(Received September 8, 2020; accepted August 16, 2021)

*Keywords:* Flexible DSSC, Binder-free TiO<sub>2</sub> paste, Fill factor, Power conversion efficiency

## 1. Introduction

As a result of increasing industrialization and the associated lifestyle, the need for energy is increasing all over the world. The silicon solar cells have been continuously advancing in efficiency but technologies of these cells are still very expensive. Research studies are being carried out on large budgets for cheaper and easier-to-manufacture solar cells. Since O'Regan and Grätzel first reported the dye-sensitized solar cell (DSSC) in 1991, DSSCs represent an attractive alternative, with the advantages of low material costs, a simple manufacturing process, desired durability, etc. [1-30]. Basically DSSC is a photo-electrochemical system in which a porous nanostructured oxide film acts as the photoanode. To increase the light absorbing capacity of the photoanode, dye molecules are adsorbed on the surface of the nanostructured oxide films. The photoanode material of DSSCs is one of the key factors affecting the photoelectric conversion efficiency [1-13]. The titanium dioxide (TiO<sub>2</sub>) has been widely used for photoanode materials because TiO<sub>2</sub> has high transparency for visible light, large value of refractive index, good adhesion, high chemical resistance, controllable specific resistance, is environmentally friendly etc. [31,32].

In order to reduce costs and make DSSC applications more practical, the development of flexible plastic sublayer based DSSCs such as PET and PEN has become necessary nowadays [14-25]. The critical challenges for plastic substrates is the requirement of low temperature annealing process, since these plastics can withstand the maximum temperature is about 150 degrees. TiO<sub>2</sub> particles cannot make high quality interconnections within themselves and with substrate due to low temperature sintering. Therefore, low-temperature titanium pastes are required for flexible photoanodes. In this paper, we were prepared a binder-free TiO<sub>2</sub> paste and the binder-free TiO<sub>2</sub> paste can provided a

good connection with flexible substrate PET/ITO at low temperatures.

## 2. Experimental

### 2.1. Materials

In this work, as a flexible conductive substrate ITO-coated Poly (ethylene terephthalate) (PET/ITO) (188 μm thick, surface resistivity 18 Ω/sq, Solaronix) was used. TiO<sub>2</sub> nanoparticles (Degussa,P25) was purchased from Sigma-Aldrich. TiO<sub>2</sub> formulation (Ti-Nanoxide T-L) and dye sensitizer Ruthenizer 535-bisTBA (one of the best ruthenium dyes for DSSCs also known as N719 in the literature) were purchased from Solaronix. 18.2 MΩ deionized water is used for cleaning procedures.

### 2.2. Binder-free TiO<sub>2</sub> paste preparation

The TiO<sub>2</sub> paste has been prepared from a mixture of a commercial TiO<sub>2</sub> powder (P25), t-butanol, DI water and commercial T-L TiO<sub>2</sub> slurry. Firstly, the TiO<sub>2</sub> pastes were prepared by dissolving 1.1 gr P25 nanoparticles in the mixed solvent of t-butanol and DI water. The high viscosity of P25 paste is due to the attractive forces dominant between the nanoparticles resulting in large agglomerates [26-28]. Then, T-L paste was added into the P25 paste and mixed using magnetic stirring for 3h. With the addition of acidic T-L into the P25 pastes, the viscosity decreases dramatically and the pastes became fluid.

### 2.3. Assembly of DSSC devices

PET/ITO substrates with dimension of 2×2 cm<sup>2</sup> were thoroughly rinsed by acetone and methanol respectively with ultrasonic bath. TiO<sub>2</sub> paste was spread onto the

prepared PET/ITO substrates by doctor blade method and drying at room temperature for 30 min. Then the film was thoroughly dried at 120° C on hot plate (20 min) and sintered at 140° C for 2 hour. The dye sensitization was performed by immersing flexible TiO<sub>2</sub> film in solution of N719 dye in ethanol at room temperature for 24 hours. The counter electrodes were used Pt/FTO (Florin doped tin oxide). The photo anodes and counter electrodes were combined with hot melt sealing film at 110 degree. Lastly, liquid electrolyte (Iodolyte HI-30, Solaronix) was injected through the thin hole in the counter electrode.

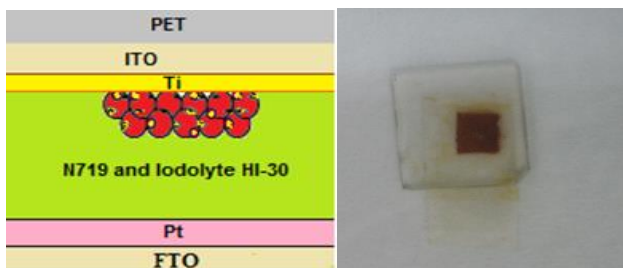


Fig. 1. Schematic of DSSC and new DSSC (color online)

## 2.4. Characterization

The as-prepared samples were characterized by X-ray diffraction (XRD) using a MP-XRD, Panalytical - Epyrean. The morphology and thickness of TiO<sub>2</sub> film were examined by scanning electron microscopy (FE-ESEM-EDS, FEI Quanta 450 FEG). Fourier transformed Raman spectroscopic measurements were performed on a Renishaw inVia Raman Microscope Spectrophotometer in

the range 4000-100 cm<sup>-1</sup> employing CCD detector. The Raman scattering was excited using 785 nm diode laser with 1% power (2.3 mW) and focused onto the samples using a 50x objective. The optical absorption spectra were recorded on a UV-vis spectrophotometer (Agilent 8453) at room temperature. The J-V curves of photovoltaic cells were measured using the Class AAA Solar Simulator (SCIENCETECH SLB-300A Compact Solar Simulator) at AM1.5G (100 mW/cm<sup>2</sup>).

## 3. Results and discussion

TiO<sub>2</sub> paste low temperature process cannot use binder materials because the binder materials need high temperature process. Therefore, in this study a binder free TiO<sub>2</sub> paste has been prepared and used for low temperature flexible DSSCs. Firstly, P25 nanoparticles have been mixed solvent of 18.2 MΩ deionized water and t-butanol. Here t-butanol was used as the surface tension reducing agent of the liquid paste to improve its adhesion to the ITO-PET surface. Then a slightly acidic T-L TiO<sub>2</sub> slurry was added into the P25 paste for a better interconnection.

### 3.1. Morphology characterization

Fig. 2 shows the SEM micrographs (different magnification) of binder free TiO<sub>2</sub> film prepared at low temperature on ITO/PET. As can be seen Fig.2, TiO<sub>2</sub> film have favorable porosity and good inter particle connection. The gaps between TiO<sub>2</sub> particles are due to low temperature annealing and the absence of special binders [33].

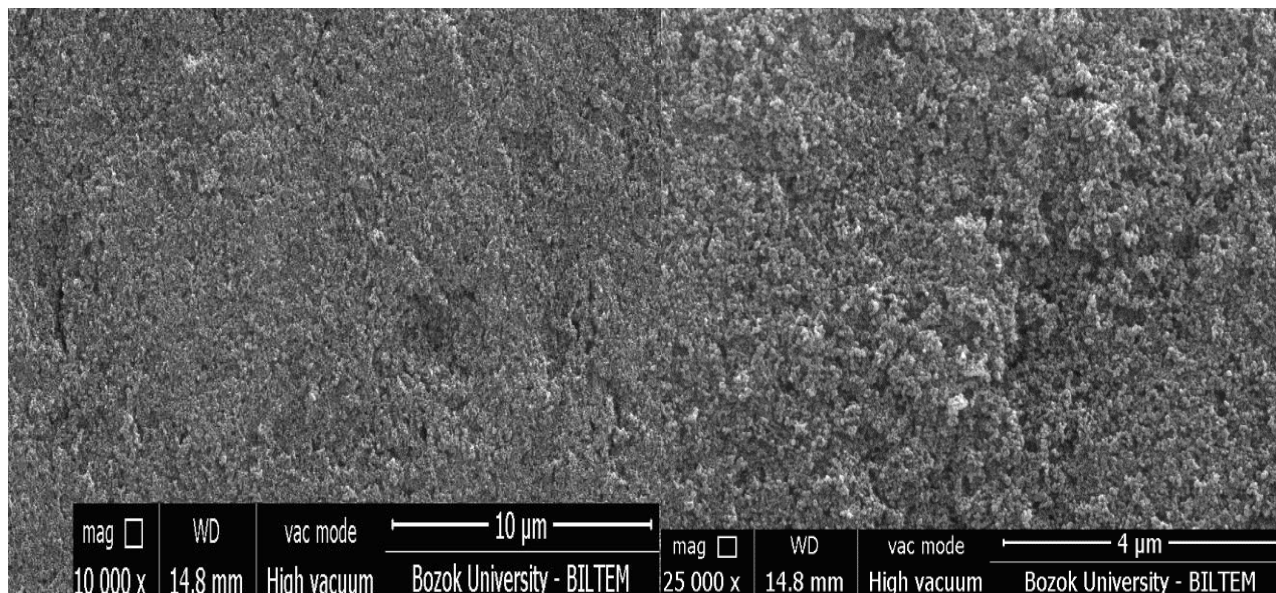


Fig. 2. SEM images of TiO<sub>2</sub> film prepared at low temperature on ITO/PET

Fig. 3 gives the EDS analysis to confirm that TiO<sub>2</sub> provides good contact to the ITO / PET surface.

Here, Ti and O peaks confirm that TiO<sub>2</sub> is coated on ITO / PET. The In and Sn peaks are ITO peaks from the gaps seen in SEM images.

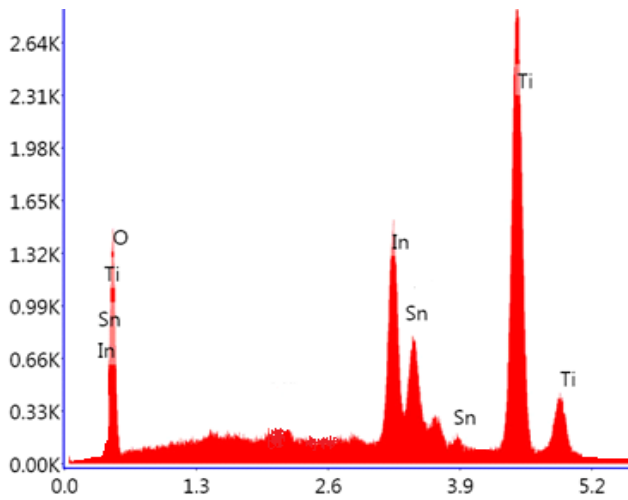
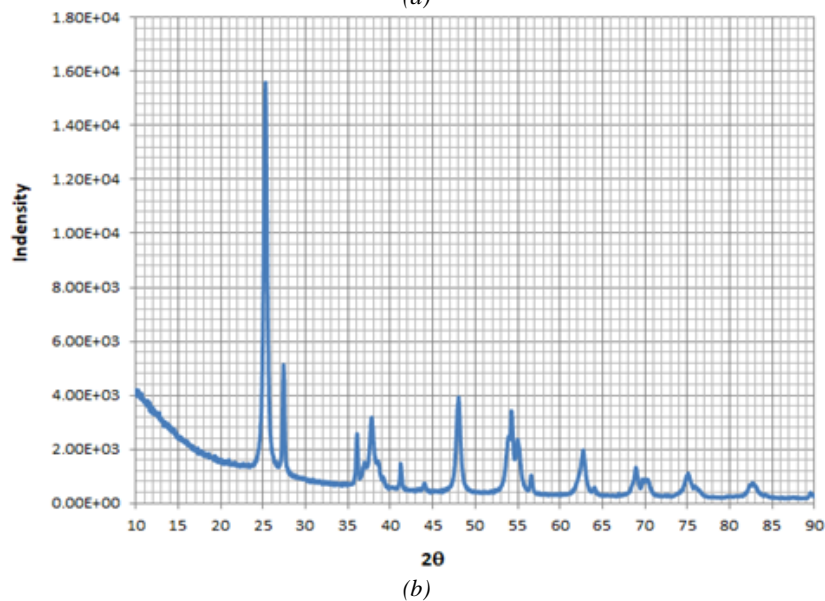
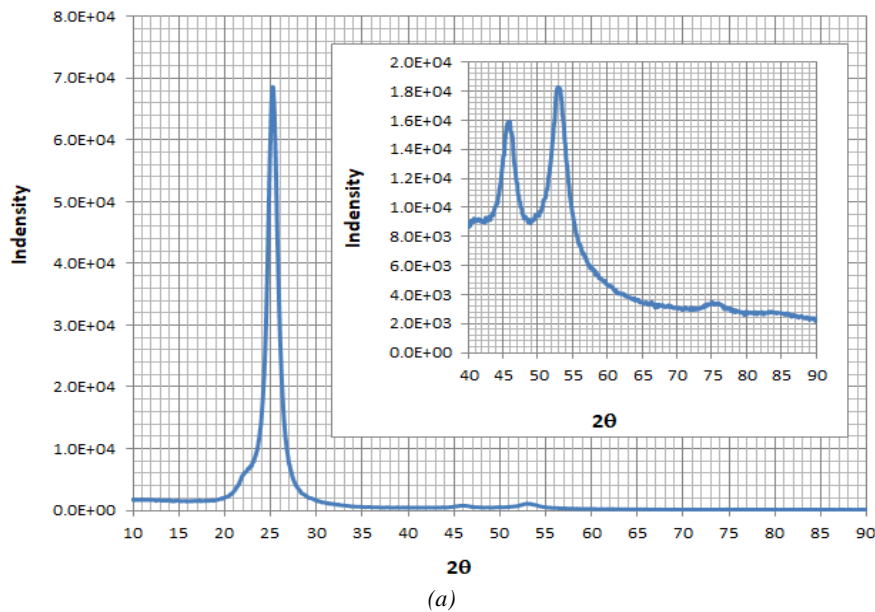


Fig. 3. EDS analysis of TiO<sub>2</sub> film prepared at low temperature on ITO/PET (color online)

### 3.2. Structural characterization

The crystal structure of TiO<sub>2</sub> films was examined by X-ray diffraction (XRD) as shown in Fig. 4. Normally Degussa P25 powder consists of phases of anatase and rutile in 4: 1 ratio. Therefore, the first paste prepared with P25 powder is crystallized in anatase and rutile phases. The commercial T-L paste is crystallized in the pure anatase phase [25-30;34]. It can be seen Fig. 4, TiO<sub>2</sub> film fabricated by the last paste exhibited crystalline phase.



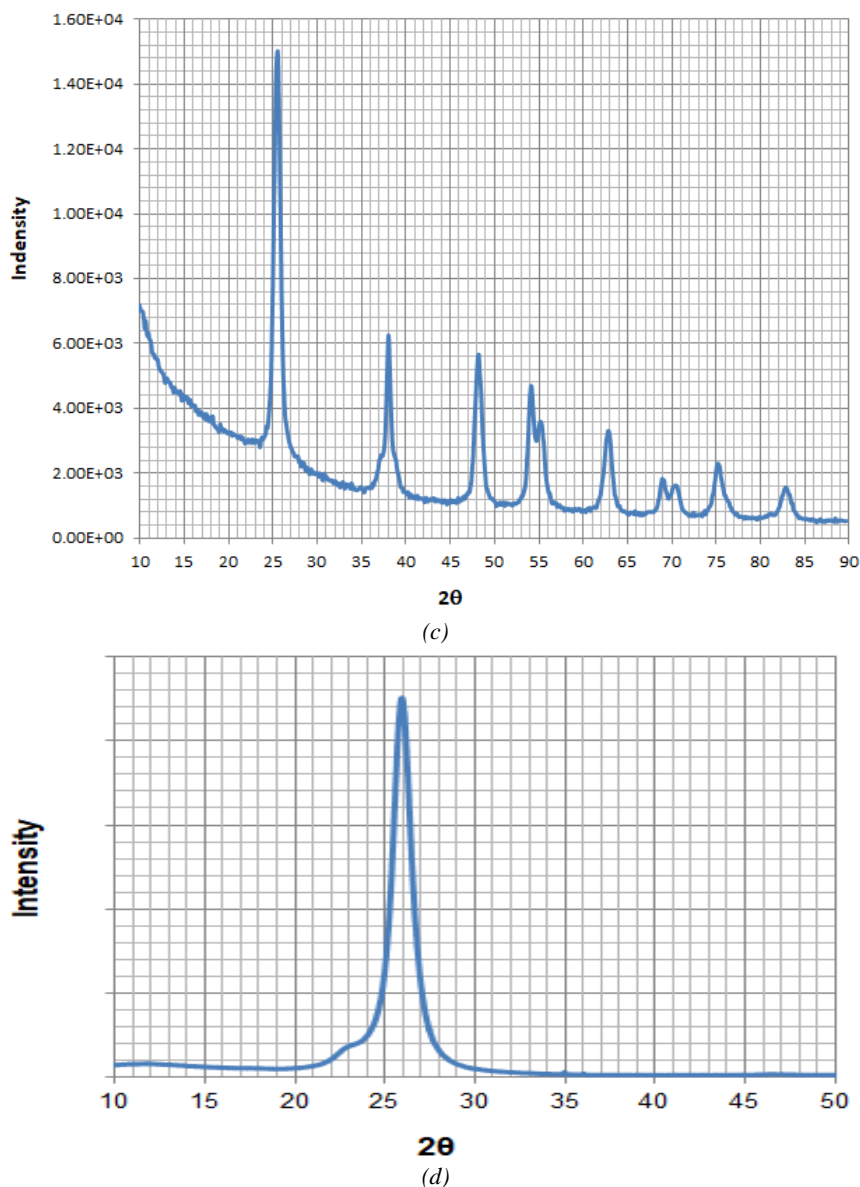


Fig. 4. (a) XRD of ITO/PET; (b) XRD of P25 nanopowder; (c) XRD of T-L paste; (d) XRD of TiO<sub>2</sub> film (color online)

The experimental Raman spectra are shown comparatively in Fig. 5. As shown in Fig. 5(a-d), the observed bands at 146, 400, 516, 640 cm<sup>-1</sup> for T-L paste were assigned to the vibration modes, E<sub>g</sub>(1), E<sub>g</sub>(2), B<sub>1g</sub>(1), A<sub>1g</sub> + B<sub>1g</sub>(2) and E<sub>g</sub>(3) for anatase TiO<sub>2</sub>, respectively in accordance with the literature [35,36]. These modes were obtained at 143, 397, 517 and 636 cm<sup>-1</sup> for the photo anode (Fig. 5d). A sharp feature observed at 143 cm<sup>-1</sup> of photo anode (anatase E<sub>g</sub> mode) was consistent with Ti-Ti covalent interaction. Broad bands observed at 397 and 517 cm<sup>-1</sup> validate Ti-O interactions, corresponding to B<sub>1g</sub> and A<sub>1g</sub> modes of anatase TiO<sub>2</sub>. The peak at 636 cm<sup>-1</sup> indicated O-O interaction with E<sub>g</sub> mode [35-37]. These results confirm the formation of anatase TiO<sub>2</sub> nanograins. The 12 bands appeared between 1730-703 cm<sup>-1</sup> in the Raman spectrum of photo anode were assigned to the vibrations of PET/ITO layer with relatively low intensities due to the screening effect of the paste layer [36,37].

Fig. 6 shows the transmission and Tauc's plot of the binder free TiO<sub>2</sub> film. The optical band gap of the prepared

TiO<sub>2</sub> film was determined by Tauc's method. The optical band gap according to the Tauc's method is obtained by the following equation.

$$(\alpha h\nu) = B(h\nu - E_g)^m \quad (4.1)$$

In this equation  $\alpha$  absorption coefficient is the energy absorbed by  $h\nu$  light, energy band gap between E<sub>g</sub> valence and conduction band, and B ratio coefficient. If the value m is known, the type of optical transition can be determined. Here m: 1/2 is the direct transition, m: 2 is the indirect transition occurs. Using equation 4.1, value of m = 0.5 was found. This indicates that the basic transition of the TiO<sub>2</sub> film is a direct transition. Using this value  $(\alpha h\nu)^2 - h\nu$  graph (Fig. 6) E<sub>g</sub> value was obtained as 3.15 eV. In the literature, similar band gap values have been obtained in TiO<sub>2</sub> films produced at low temperatures [41].

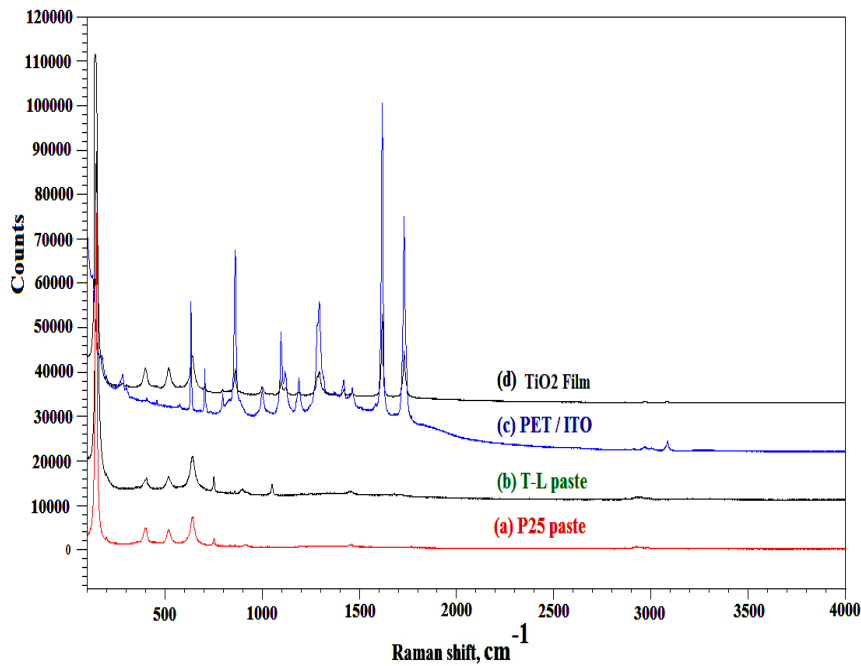


Fig. 5. Raman spectra of a) P25 paste b) T-L paste, c) PET/ITO d) photo anode (color online)

### 3.3. Photovoltaic properties

Finally, the photoelectrode and Pt electrode were combined and photovoltaic parameters of flexible DSSC were examined. Fig. 7 shows the experimental forward bias J-V characteristics of DSSC at AM1.5G (100 mW/cm<sup>2</sup>) simulated sunlight. The characteristic values of short circuit photocurrent ( $J_{sc}$ ), open-circuit voltage ( $V_{oc}$ ), fill factor (FF) and conversion efficiency ( $\eta$ ) for the flexible DSSC were calculated using the following equation.

$$FF = \frac{V_{max} \times I_{max}}{V_{oc} \times I_{sc}} \quad (4.2)$$

$$\eta = \frac{V_{oc} \times I_{sc} \times FF}{P_{input power}} \quad (4.3)$$

The calculated values of  $J_{sc}$ ,  $V_{oc}$ , FF and  $\eta$  are 20.9 mA/cm<sup>2</sup>, 671 mV, 0.57, and 7.95 % respectively. The flexible photoanode prepared by low temperature TiO<sub>2</sub> paste has favorable particle inter connection structure and high adhesion between the film and substrate which facilitates the electron transport efficiency and improves the  $J_{sc}$  of DSSC. The resulting J-V characteristics of DSSC are consistent with the results of DSSC produced with similar TiO<sub>2</sub> pastes [38-40]. The low-temperature titanium pastes are required for flexible photoanodes. However, The TiO<sub>2</sub> paste based on the low temperature method shows slight lower conversion efficiency than that fabricated by conventional high temperature sintering method due to its slower electron transport rate and larger inherent resistance. Further studies are required using lower resistivity plastic substrates [25-30,33,38-40].

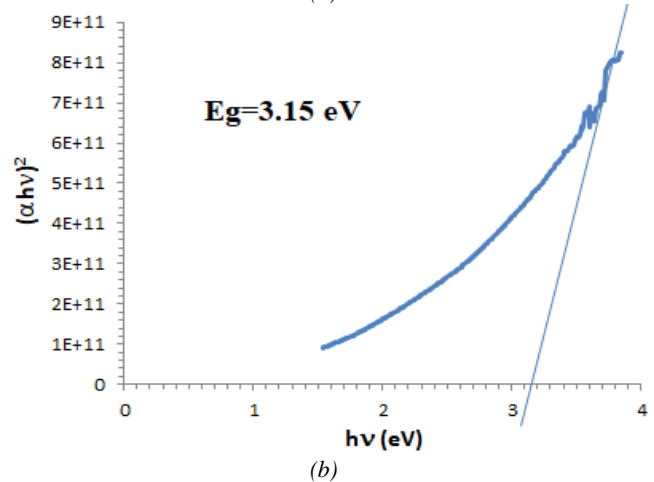
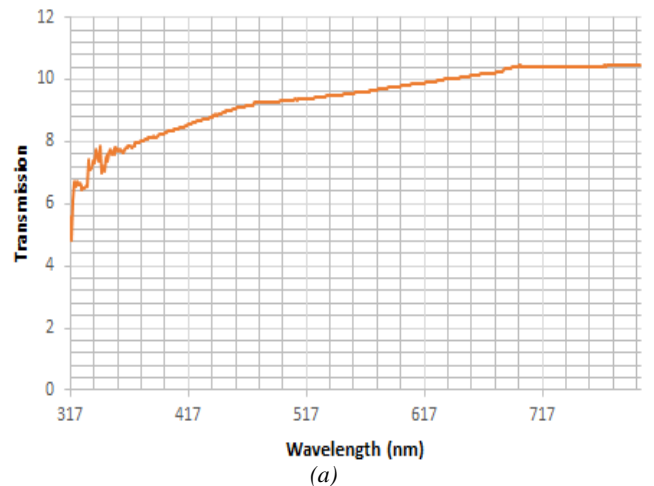


Fig. 6. (a) Transmission spectra; (b) Tauc's Plot TiO<sub>2</sub> film (color online)

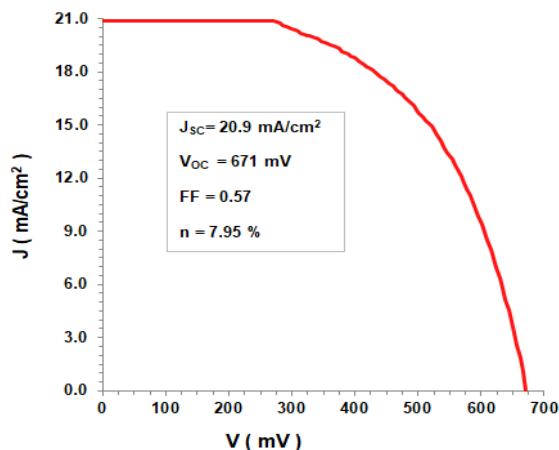


Fig. 7. *J-V characteristics of DSSC that was fabricated with the low temperature TiO<sub>2</sub> paste (color online)*

#### 4. Conclusions

In this study, DSSCs were produced using low temperature procedures due to the use of flexible ITO / PET substrates. The methods using low-temperature procedure should overcome two main problems for improving the photovoltaic performance. First problem is the incomplete connection of TiO<sub>2</sub> particles. Second problem is the residuals of the organic binder within the TiO<sub>2</sub> film. An organic binder is usually added during the preparation of a porous TiO<sub>2</sub> film for a DSSC. The residual of the binder in a low temperature process (< 450 degree) would become an insulating core and block the transporting path of electrons. For the above mention reasons, a binder-free and suitable for low temperature annealing TiO<sub>2</sub> paste was prepared and used. XRD measurements of this paste were shown that TiO<sub>2</sub> film fabricated by this paste exhibited crystalline phase. Also SEM measurements of this paste were shown that TiO<sub>2</sub> film have favorable porosity and good inter particle connection. Therefore, the prepared film was used in the production of DSSC. The values  $J_{sc}$ ,  $V_{oc}$ , FF and  $\eta$  of the flexible DSSC calculated as 20.09 mA/cm<sup>2</sup>, 671 mV, 0.57, and 7.95 % respectively.

#### Acknowledgments

This work was supported by The Management Unit of Scientific Research Project of Yozgat Bozok University (6602c-FEF/17-65). We would like to thank Yozgat Bozok University Science & Technology Application and Research Center for XRD, SEM and Solar simulator measurements and we would like to thank Prof. Dr. Hidayet Cetin, Associate Prof. Dr. Ali Delibas and Dr. Mucalla Ozbay Karakuş, Dr. Hatice Arı for contributions.

#### References

[1] B. O' Regan, M. Grätzel, *Nature* **353**(6346), 737 (1991).

- [2] M. Grätzel, *Proc. Indian Acad. Sci.* **107**(6), 607 (1995).
- [3] A. Hagfeldt, M. Grätzel, *Chem.Rev.* **95**(1), 49 (1995).
- [4] K. Kalyanasundaram, M. Grätzel, *Coordination Chemistry Reviews* **177**(1), 347 (1998).
- [5] N. S. Sariciftci, L. Smilowitz, A. J. Heeger, F. Wudl, *Science* **258**(5087), 1474 (1992).
- [6] A. Kay, M. Grätzel, *J. Phys. Chem.* **97**(23), 6272 (1993).
- [7] MD. K. Nazeeruddin, R. Humphry-Baker, M. Grätzel et al., *J. Porphyrins Phthalocyanines* **3**, 230 (1999).
- [8] J. Gong, J. Liang, K. Sumathy, *Renewable and Sustainable Energy Reviews* **16**(8), 5848 (2012).
- [9] A. Islam et al., *J. Photochem. Photobiol. A* **158**, 131 (2003).
- [10] K. Hara et al., *New J. Chem.* **27**(5) 783 (2003).
- [11] C. Wu, E. Jia et al., *ACS Appl. Mater. Interface* **5**(16), 7886 (2013).
- [12] Y. Zhang, B. Zhang, X. Peng, L. Liu et al., *Nano Research* **8**(12), 3830 (2015).
- [13] S. Kiran, S. K. Naveen Kumar, K. C. Yogananda, Dinesh Rangappa, *Journal of Materials Science: Materials in Electronics* **29**(15), 12681 (2018).
- [14] L. Chen et al., *Electrochimica Acta* **55**, 3721 (2010).
- [15] Y. Han, J. M. Pringle, Y. B. Cheng, *Photochemistry and Photobiology* **91**, 315 (2015).
- [16] W. Huang, X. L. Zhang, F. Huang, Z. Zhang et al., *J. Nanopart. Res.* **14**, 838 (2012).
- [17] T. A. Nirmal Peiris, S. Senthilarasu et al., *Phys. Chem. C* **116**, 211 (2012).
- [18] X. Yin, Z. Xue, L. Wang, Y. Cheng, B. Liu, *ACS Appl. Mater. Interfaces* **4**, 1709 (2012).
- [19] J. Shao, F. Liu, W. Dong, R. Tao, Z. Deng, X. Fang, S. Dai, *Materials Letters* **68**, 493 (2012).
- [20] W. H. Chiu, K. M. Lee, W. F. Hsieh, *Journal of Power Sources* **196**, 3683 (2011).
- [21] C. H. Lee, W. H. Chiu, K. M. Lee, W. F. Hsieh, J. M. Wu, *J. Mater. Chem.* **21**, 5114 (2011).
- [22] K. Fan, C. Gong, T. Peng, J. Chen, J. Xia, *Nanoscale* **3**, 3900(2011).
- [23] Y. W. Jang, Y. K. Kim, H. W Park, D. H. Won, S. E. Cho, W. P. Hwang, K. S. Jung et al., *Mol. Cryst. Liq. Cryst.* **538**, 240 (2011).
- [24] Q. Zeng, Y. Yu, L. Wu, B. Qi, J. Zhi, *Phys. Status Solidi A* **207**, 2201 (2010).
- [25] Lu-Yin Lin, Po-Chin Nien, Chuan-Pei Lee, Keng-Wei Tsai, Min-Hsin Yeh, R. Vittal, Kuo-Chuan Ho, *J. Phys. Chem. C* **114**, 21808 (2010).
- [26] X. Zhao, P. Yang et al., *Electrochim. Acta* **146**, 164 (2014).
- [27] Y. Kijitori, M. Ikegami, T. Miyasaka, *Chem. Lett.* **36**, 190 (2017).
- [28] G. Syrokostas, G. Leftheriotis, P. Yianoulis, *Renew. Energy* **72**, 164 (2014).
- [29] P. M. Sommeling et al., *J. Phys. Chem. B* **110**, 19191 (2006).
- [30] T. W. Hamann et al., *Energy Environ. Sci.* **1**, 66 (2008).
- [31] S. A. Kazmi, S. Hameed, A. Azam, *Energy Sources, part A: Recovery, Utilization, and Environmental*

- Effects **39**, 67 (2017).
- [32] M. Houshmand, H. Esmaili, M. H. Zandi, N. E. Gorji, *Mater. Let.* **157**, 123 (2015).
- [33] H. C. Weerasinghe, F. Huang, Y. B. Cheng, *Nano Energy* **2**, 174 (2013).
- [34] H. Chang, T. L. Chen, K. D. Huang, S. H. Chien, K. C. Hung, *Journal of Alloys and Compounds* **504**, 435 (2010).
- [35] M. Giarola, A. Sanson, F. Monti, G. Mariotto, *Physical Review B* **81**, 174305 (2010).
- [36] M. Grujić-Brojčin, M. Šćepanović, Z. Dohčević- Mitrović, Z. V. Popović, *Science of Sintering* **38**, 183 (2006).
- [37] F. D. Hardcastle, H. Ishihara et al., *J. Mater. Chem.* **21**, 6337 (2011).
- [38] K. Fana, T. Peng, J. Chena, K. Daia, *Journal of Power Sources* **196**, 2939(2011).
- [39] P. Zhang, C. Wu, Y. Han, T. Jin, B. Chi, J. Pu, L. Jian, *J. Am. Ceram. Soc.* **95**, 1372 (2012).
- [40] C. Cheng, J. Wu, Y. Xiao, Y. Chen, L. Fan et al., *Electrochimica Acta* **56**, 7256 (2011).
- [41] M. Sabet, H. Jahangiri, *J. Mater. Sci: Mater. Electron.* **29**, 778 (2018).

---

\*Corresponding author: hatice.kanbur@bozok.edu.tr